

University of California Santa Cruz
Baskin School of Engineering
Electrical Engineering Department

Boost Converter Project Final Report

Matthew Randall

9 June 2025

ECE 177L
Instructor: Keith Corzine

1 Abstract

This project investigates the theoretical, simulated, and measured behavior of a boost converter operating in both continuous conduction mode (CCM) and discontinuous conduction mode (DCM). Electrical parameters such as output voltage, inductor current, ripple, and efficiency were derived analytically and compared to MATLAB Simulink simulations and experimental measurements. By varying load resistance and inductor resistance, the converter's performance was evaluated under different operating conditions. Transient behavior was also explored using a microcontroller-based feedback loop to regulate output voltage under step changes in load and reference voltage. Results show that theoretical predictions for current and efficiency are accurate. Experimental results closely matched simulations, validating the analytical models and highlighting design considerations for stable and efficient converter operation.

2 Boost Converter Theory

A boost converter is a type of DC-DC power converter that steps up the input voltage to a higher output voltage. It operates by storing energy in an inductor during the switch-on phase and releasing it to the output during the switch-off phase. The energy transfer is controlled by a switch, typically a MOSFET, and a diode to direct current flow during off phases. The converter operates in continuous conduction mode (CCM) when the inductor current never falls to zero, and in discontinuous conduction mode (DCM) when the inductor current reaches zero before the end of a switching cycle.

In the ideal case (neglecting resistive losses), the output voltage in CCM is given by:

$$V_{o,\text{ideal}} = \frac{V_s}{1 - D} \quad (1)$$

where V_s is the input voltage and D is the duty cycle.

To account for power losses due to the inductor's resistance r_L , the actual output voltage is:

$$V_o = \frac{V_s}{1 - D} \cdot \left(1 + \frac{r_L}{(1 - D)^2 R}\right)^{-1} \quad (2)$$

where R is the load resistance.

The average inductor current under CCM is:

$$I_L = \frac{V_o}{(1 - D)R} \quad (3)$$

The peak-to-peak ripple of the inductor current is:

$$\Delta i_L = \frac{D(1 - D)TV_o}{L} \quad (4)$$

where $T = \frac{1}{f}$ is the switching period, f is the switching frequency, and L is the inductance.

Assuming a triangular waveform for inductor current ripple:

$$I_{L,\max} = I_L + \frac{\Delta i_L}{2} \quad (5)$$

$$I_{L,\min} = I_L - \frac{\Delta i_L}{2} \quad (6)$$

To account for power dissipation, the RMS current through the inductor is:

$$I_{L,\text{rms}} = \sqrt{I_L^2 + \frac{(\Delta i_L)^2}{12}} \quad (7)$$

The relative output voltage error compared to the ideal case is:

$$\text{Vo Error} = \frac{V_{o,\text{ideal}} - V_o}{V_o} \quad (8)$$

The efficiency of the converter, accounting only for conduction losses in the inductor, is:

$$\eta = 1 - \frac{P_{loss}}{P_s} = 1 - \frac{I_{L,rms}^2 r_L}{V_s I_L} \quad (9)$$

Discontinuous Conduction Mode (DCM) Equations:

The DCM output voltage is:

$$V_o = \left(\frac{D + D_1}{D_1} \right) V_s \quad (10)$$

Where D_1 is given by:

$$D_1 = \frac{L}{RDT} + \frac{1}{2} \sqrt{\left(\frac{4L^2}{R^2 D^2 T^2} + \frac{8L}{RT} \right)} \quad (11)$$

The voltage ripple across the output is:

$$\Delta V_o = \left(\frac{(2 - D_1)^2 T^2}{8LC} \right) \left(\frac{DD_1^2}{D + D_1} \right) V_o \quad (12)$$

The average inductor current:

$$I_L = \frac{DD_1 TV_o}{2L} \quad (13)$$

Maximum inductor current:

$$I_{\max} = \frac{DD_1 V_o T}{(D + D_1)L} \quad (14)$$

Minimum inductor current:

$$I_{\min} = 0 \quad (15)$$

These equations enable the analysis of a boost converter in both CCM and DCM. The goal of this project is to compare the boost converter equations, a Simulink simulated boost converter and an in lab built boost converter.

3 Simulation Set Up

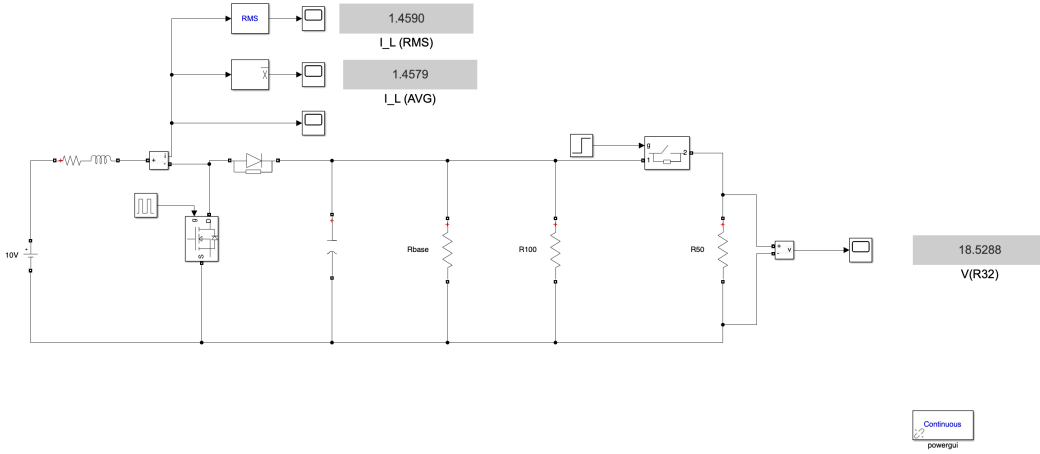


Figure 1: Simulation Set Up for Boost Converter

Figure 1 shows the schematic of the simulated boost converter. The boost converter circuit was simulated using Matlab's Simulink specialized power library to evaluate its steady-state switching behavior.

The parameters used in the simulation are summarized in Table 1.

Component	Value
Input Voltage V_{in}	10 V
Switching Frequency f	20 kHz
Inductance L	1.5 mH
Capacitance C	470 μ F
Duty Cycle D	60%

Table 1: Simulation parameters for the boost converter.

The circuit in Figure 1 was analyzed using the built in voltage and current probes in Simulink. The inductor resistance was changed from 0.375 to 1.5Ω and load resistance was changed from 1000 , 90.9 , and 32.3Ω . The output behavior of the boost converter was observed for each resistance case. In addition, the inductor current behavior and efficiency was also compared to calculated values. All calculated values come from Equations 1-9.

4 Simulation Results

First the simulated values for $r_L = 0.375\Omega$ were compared to calculated values for each case of R_o . This is shown in Tables 2-4.

$R_o = 1000\Omega$	Calculated (DCM)	Simulation
V_o	30.000	25.8
$V_{o,error}$	—	14%
I_L	0.090	0.100
I_{max}	0.200	0.204
I_{min}	0	0
$I_{L,rms}$	0.112	0.122
Efficiency	99.47%	99.44%

Table 2: Simulation results for DCM with $R_o = 1000\Omega$ and $r_L = 0.375\Omega$

$R_o = 90.9 \Omega$	Calculated	Simulation
V_o	24.267	23.48
$V_{o,error}$	2.57%	6.47%
I_L	0.677	0.674
I_{\max}	0.774	0.768
I_{\min}	0.579	0.577
$I_{L,\text{rms}}$	0.679	0.678
Efficiency	97.44%	97.44%

Table 3: Simulation results for $R_o = 90.9 \Omega$ and $r_L = 0.375 \Omega$

$R_o = 32.3 \Omega$	Calculated	Simulation
V_o	23.312	22.32
$V_{o,error}$	7.23%	12%
I_L	1.804	1.755
I_{\max}	1.897	1.854
I_{\min}	1.711	1.655
$I_{L,\text{rms}}$	1.805	1.758
Efficiency	93.23%	93.39%

Table 4: Simulation results for $R_o = 32.3 \Omega$ and $r_L = 0.375 \Omega$

Next the simulated values for $r_L = 1.5 \Omega$ were compared to calculated values for each case of R_o . This is shown in Tables 5-7.

$R_o = 1000 \Omega$	Calculated (DCM)	Simulation
V_o	30	25.59
$V_{o,error}$	—	14.7%
I_L	0.090	0.100
I_{\max}	0.200	0.197
I_{\min}	0	0
$I_{L,\text{rms}}$	0.112	0.123
Efficiency	97.91%	97.30%

Table 5: Simulation results for $R_o = 1000 \Omega$ and $r_L = 1.5 \Omega$

$R_o = 90.9 \Omega$	Calculated	Simulation
V_o	22.64	21.76
$V_{o,error}$	9.44%	12.96%
I_L	0.628	0.626
I_{\max}	0.720	0.720
I_{\min}	0.538	0.538
$I_{L,\text{rms}}$	0.631	0.630
Efficiency	90.49%	90.49%

Table 6: Simulation results for $R_o = 90.9 \Omega$ and $r_L = 1.5 \Omega$

$R_o = 32.3 \Omega$	Calculated	Simulation
V_o	19.38	18.53
$V_{o,\text{error}}$	22.48%	25.88%
I_L	1.500	1.458
I_{\max}	1.577	1.544
I_{\min}	1.422	1.370
$I_{L,\text{rms}}$	1.500	1.459
Efficiency	77.50%	78.50%

Table 7: Simulation results for $R_o = 32.3 \Omega$ and $r_L = 1.5 \Omega$

5 Analysis of Simulation Results

The simulated values for $r_L = 0.375 \Omega$ were first compared to theoretical calculations across three load conditions: $R_o = 1000 \Omega$, 90.9Ω , and 32.3Ω . For the high-load case ($R_o = 1000 \Omega$), the converter operates in discontinuous conduction mode (DCM). The calculated output voltage in this case assumes an ideal model without accounting for inductor resistance, which explains the difference between the calculated and simulated result. Despite this, the inductor current values and efficiency remained closely aligned, indicating that power transfer and current waveforms were accurately predicted by the theoretical model. As the load resistance decreased, the converter transitioned to continuous conduction mode (CCM), and the output voltage predictions became more accurate. Voltage error remained under 8% in all CCM cases, and current and efficiency values showed agreement with simulation.

The second set of comparisons was performed for $r_L = 1.5 \Omega$. Across all load conditions, the increased inductor resistance led to larger output voltage errors, particularly in the DCM case. For $R_o = 1000 \Omega$, the ideal DCM model

again significantly overestimated V_o , reinforcing the importance of including r_L in low-current DCM analysis. Under heavier loads, the impact of r_L was more pronounced, resulting in reduced efficiency and voltage drops. However, the current predictions remained accurate. Overall, the simulations confirm that inductor resistance and load level are critical factors in converter performance, especially in DCM.

6 Microprocessor Programming

Next the Microprocessor was programmed using the Simulink Support Package for Arduino Hardware. Figure 2 shows the simulation diagram used to program the Arduino.

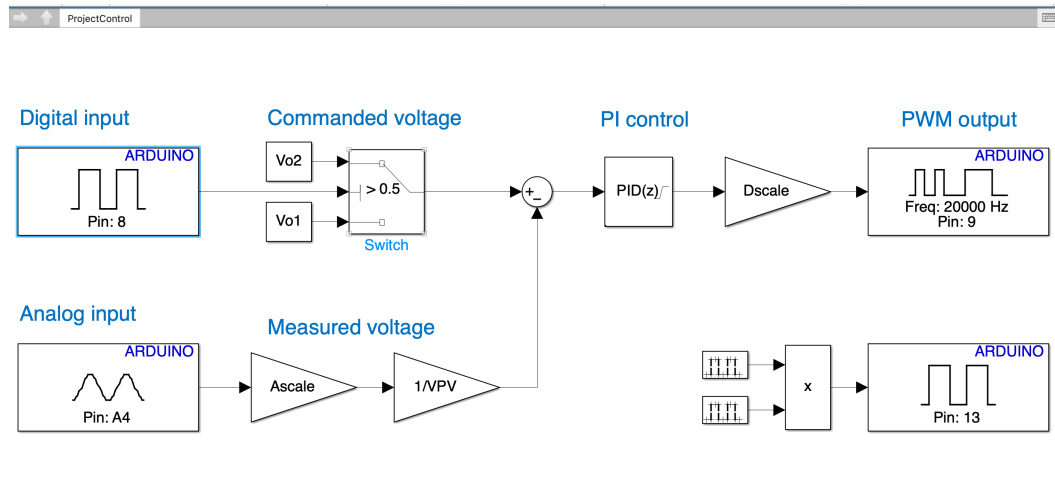


Figure 2: Simulation diagram used to program the Arduino

Next the code was built and run on the Arduino, Figure 3 shows the output diagnostics.

The screenshot shows the Diagnostic Viewer interface. At the top, it displays build statistics: ".text + .data + .bss" totaling 382 bytes (18.7% Full), deployment to an Arduino Uno on port COM3, successful code deployment, and a successful build procedure for "ProjectControl0x2810x29". Below this, a message states "Build process completed successfully". A "Build Summary" section is expanded, showing a table of model targets:

Model	Build Reason	Status	Build Duration
ProjectControl0x2810x29	Target (ProjectControl0x2810x29.c) did not exist. Code generated and compiled.	0h 0m 47.246s	

Summary statistics: 1 of 1 models built (0 models already up to date). Build duration: 0h 0m 53.479s.

Figure 3: Diagnostics of built code on the Arduino

From Figure 3, the diagnostics indicate that the code was built and executed without errors. This was my first time programming an Arduino, and the process using the Simulink Support Package for Arduino Hardware followed a clear sequence of steps. I have previously programmed other microprocessors in C, which required manual configuration of hardware registers, setup of development environments, and low-level debugging. In comparison, the workflow through Simulink involved fewer manual steps and allowed for direct deployment of the code. This approach demonstrated a method for programming embedded systems without relying on traditional code.

7 Measurement Setup

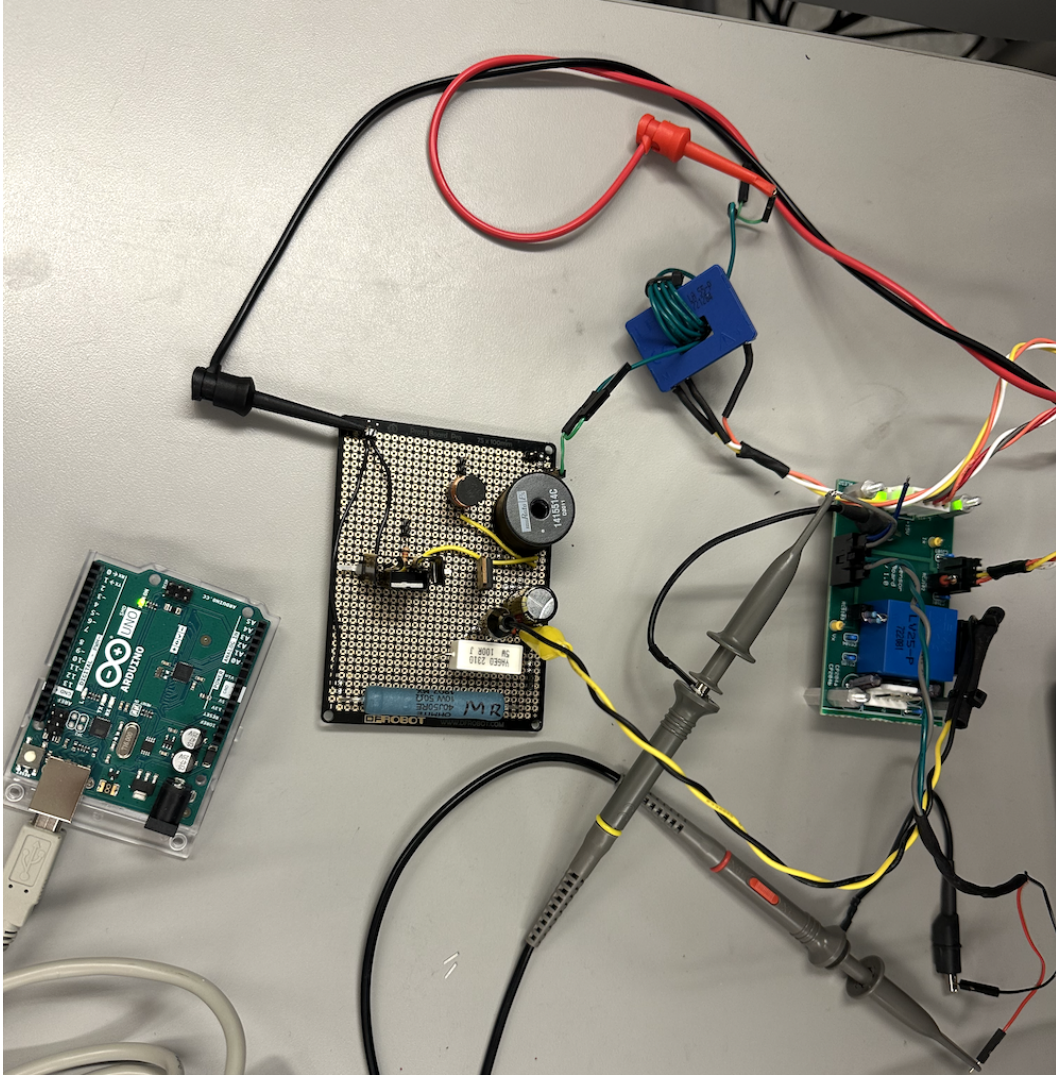


Figure 4: Photo of the boost converter measurement setup

Figure 4 shows the measurement setup used to test the built boost converter. The boost converter was connected to a special built current probe that converts the current to volts to be displayed on the oscilloscope. The boost converter was tested using a combination of steady-state and transient measurement.

For steady-state analysis, the large inductor and base load were used initially. The duty cycle was programmed through an Arduino using the

provided `ProjectControl12.slx` Simulink file. The model was configured with $D_{max} = 0.6$ and $D_{min} = 0.999 \times D_{max}$, resulting in a constant duty cycle. The Arduino output was connected to the MOSFET gate driver of the boost converter.

Measurements were taken under the same three loading conditions as the simulation: the base load, base load plus a 100Ω resistor, and base load plus a 50Ω resistor. These tests were repeated using the smaller inductor to observe changes in converter behavior.

For transient measurements, the Arduino controller in Figure 2 was configured for feedback operation. The Simulink file was modified with $D_{max} = 0.8$, $D_{min} = 0.1$, $K_p = 0$, and $K_i = 0.2$. Commanded output voltages were set to 15 V and 25 V, with voltage sensing gain $VPV = 0.1$. The analog feedback signal was connected to pin A4 of the Arduino. Transients were triggered by toggling pin 8 between ground and +3.3 V which switches the desired output voltage from 15 V to 25 V. Another transient was captured by connecting and disconnecting the 50Ω load. Oscilloscope captures were taken for both voltage step and load change conditions.

Finally, the controller was reprogrammed with a high integral gain of $K_i = 200$ and tested again under a 25 V output target with the 50Ω load to observe regulation behavior with more aggressive feedback.

8 Measurement Results

8.1 Steady State Analysis

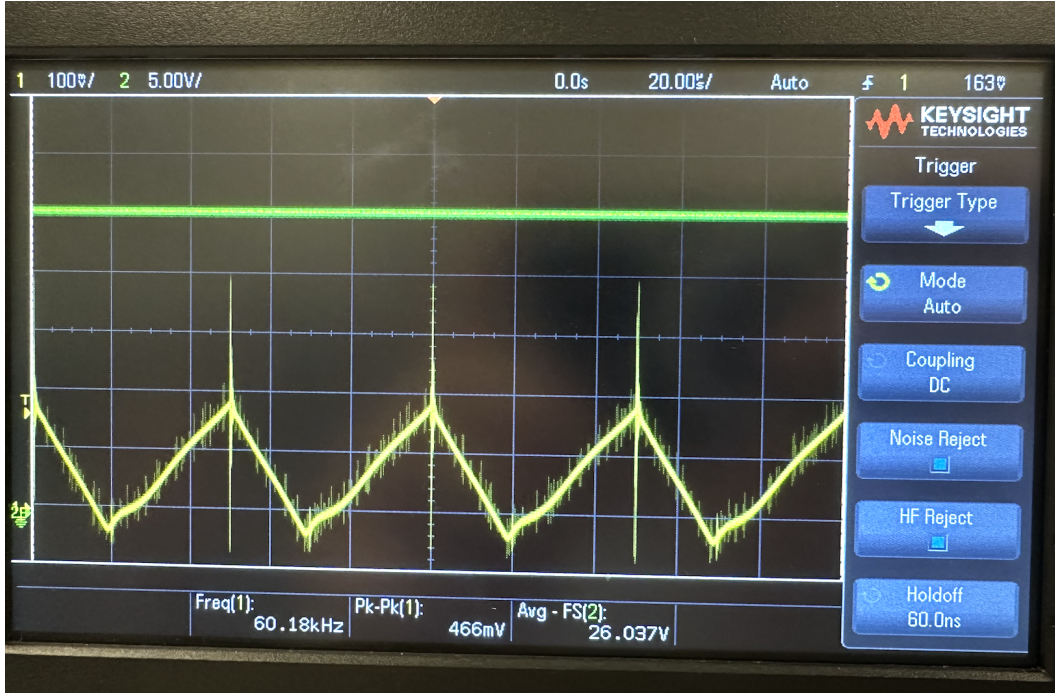


Figure 5: Photo of the boost converter output for $R_o = 1000 \Omega$ and $r_L = 0.375 \Omega$

Figure 5 shows the oscilloscope waveform for the boost converter under the $R_o = 1000 \Omega$ and $r_L = 0.375 \Omega$ load condition. The green waveform shows the output voltage and the yellow waveform shows the input current. Under this load condition, the boost converter is operating in discontinuous mode, so the yellow waveform drops to zero. The spikes on the current waveform are unfiltered high frequency transients from the mosfet switching.

Next the simulated data was compared to the measured data for the boost converter, this is shown in Tables 8-13. Tables 8-10 show the data for $r_L = 0.375 \Omega$ and Tables 11-13 show the data for $r_L = 1.5 \Omega$.

$R_o = 1000 \Omega$	Calculated (DCM)	Simulation	Measured
V_o	30.000	25.8	26.1
$V_{o,error}$	—	14%	13%
I_L	0.090	0.100	0.073
I_{\max}	0.200	0.204	0.176
I_{\min}	0	0	0
$I_{L,\text{rms}}$	0.112	0.122	0.097
Efficiency	99.47%	99.44%	99.51%

Table 8: Measurement results for DCM with $R_o = 1000 \Omega$ and $r_L = 0.375 \Omega$

$R_o = 90.9 \Omega$	Calculated	Simulation	Measured
V_o	24.267	23.48	23.6
$V_{o,error}$	2.57%	6.47%	5.6%
I_L	0.677	0.674	0.639
I_{\max}	0.774	0.768	0.73
I_{\min}	0.579	0.577	0.54
$I_{L,\text{rms}}$	0.679	0.678	0.642
Efficiency	97.44%	97.44%	97.60%

Table 9: Measurement results for $R_o = 90.9 \Omega$ and $r_L = 0.375 \Omega$

$R_o = 32.3 \Omega$	Calculated	Simulation	Measured
V_o	23.312	22.32	21.2
$V_{o,\text{error}}$	7.23%	12%	15.2%
I_L	1.804	1.755	1.65
I_{\max}	1.897	1.854	1.73
I_{\min}	1.711	1.655	1.57
$I_{L,\text{rms}}$	1.805	1.758	1.65
Efficiency	93.23%	93.39%	93.83%

Table 10: Measurement results for $R_o = 32.3 \Omega$ and $r_L = 0.375 \Omega$

$R_o = 1000 \Omega$	Calculated (DCM)	Simulation	Measured
V_o	30	25.59	25.5
$V_{o,\text{error}}$	–	14.7%	15%
I_L	0.090	0.100	0.071
I_{\max}	0.200	0.197	0.176
I_{\min}	0	0	0
$I_{L,\text{rms}}$	0.112	0.123	0.094
Efficiency	97.91%	97.30%	98.13%

Table 11: Measurement results for $R_o = 1000 \Omega$ and $r_L = 1.5 \Omega$

$R_o = 90.9 \Omega$	Calculated	Simulation	Measured
V_o	22.64	21.76	22
$V_{o,error}$	9.44%	12.96%	12%
I_L	0.628	0.626	0.603
I_{\max}	0.720	0.720	0.685
I_{\min}	0.538	0.538	0.507
$I_{L,\text{rms}}$	0.631	0.630	0.605
Efficiency	90.49%	90.49%	90.89%

Table 12: Measurement results for $R_o = 90.9 \Omega$ and $r_L = 1.5 \Omega$

$R_o = 32.3 \Omega$	Calculated	Simulation	Measured
V_o	19.38	18.53	17.7
$V_{o,error}$	22.48%	25.88%	29.2%
I_L	1.500	1.458	1.39
I_{\max}	1.577	1.544	1.85
I_{\min}	1.422	1.370	1.01
$I_{L,\text{rms}}$	1.500	1.459	1.42
Efficiency	77.50%	78.50%	78.24%

Table 13: Measurement results for $R_o = 32.3 \Omega$ and $r_L = 1.5 \Omega$

Across all test cases, the simulated and measured results aligned with the calculated values, validating the analytical models for both DCM and CCM operation. As expected, decreasing the load resistance R_o resulted in lower output voltage and efficiency. Efficiency remained high across all configurations, exceeding 97% for both low and high load resistances when $r_L = 0.375 \Omega$. The current waveforms also followed expected trends, with I_{\max} and $I_{L,\text{rms}}$ tracking closely across calculation, simulation, and measurement.

The efficiency for the measured boost converter was somehow higher than both the simulation and calculations, this is probably due to slight changes in the current measurements having a large effect in Equation 9.

When the inductor resistance increased to $r_L = 1.5 \Omega$, performance degradation became more apparent. The output voltage dropped more significantly at lower load resistances, and voltage error increased, peaking at 29.2% for $R_o = 32.3 \Omega$. This behavior is attributed to the increased voltage drop across the inductor and higher conduction losses. Current ripple also became more pronounced, especially under high load, where the measured I_{min} fell to 1.01 A, indicating reduced regulation. Efficiency decreased to 78.24% when $R_o = 32.3 \Omega$, showing the impact of inductor resistance on maintaining converter performance under heavier loads.

Lastly under the final condition, $R_o = 32.3 \Omega$ and $r_L = 1.5 \Omega$, The inductor exceeds its maximum rated current. The impact of this is shown in Figure 6.

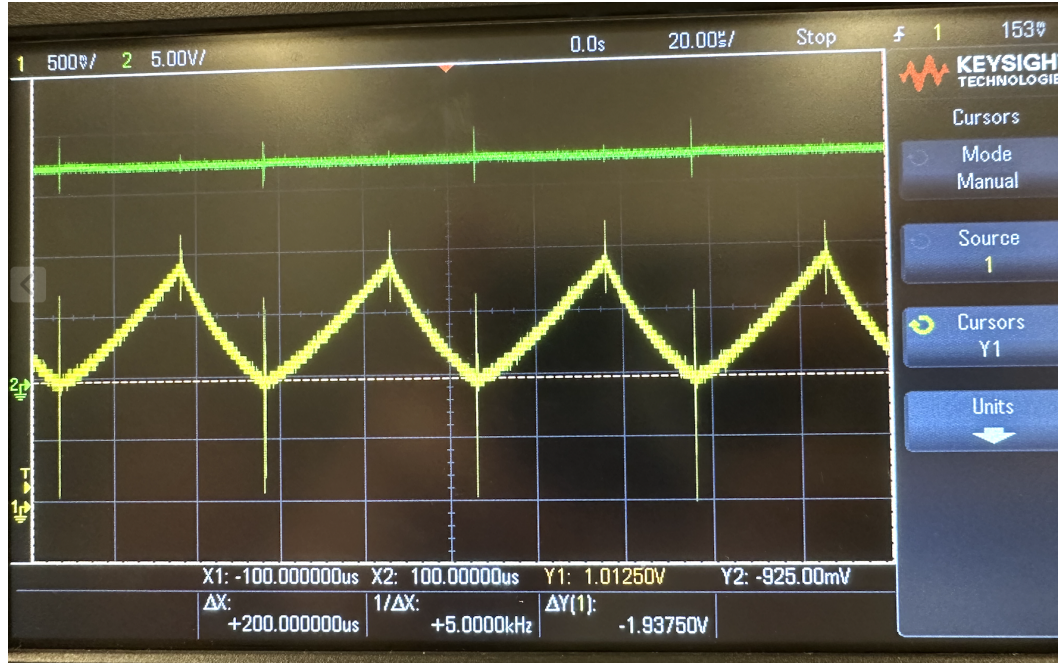


Figure 6: Measured voltage and current waveforms when current exceeds inductors maximum rating, $R_o = 32.3 \Omega$ and $r_L = 1.5 \Omega$

From Figure 6, when the inductor current exceeds its maximum rated value, the waveform begins to smooth out due to magnetic core saturation. In this saturated state, the inductor loses its ability to effectively oppose changes in current, resulting in a linear rise in current. Additionally, the inductor experiences significant heating under these conditions and may overheat or become damaged if the high current persists for too long.

8.2 Transient Analysis

First, the transient waveform was observed when pin 8 was switched from ground to 3.3 V. This changes the desired output from 15 V to 25 V. The result is shown in Figure 7.

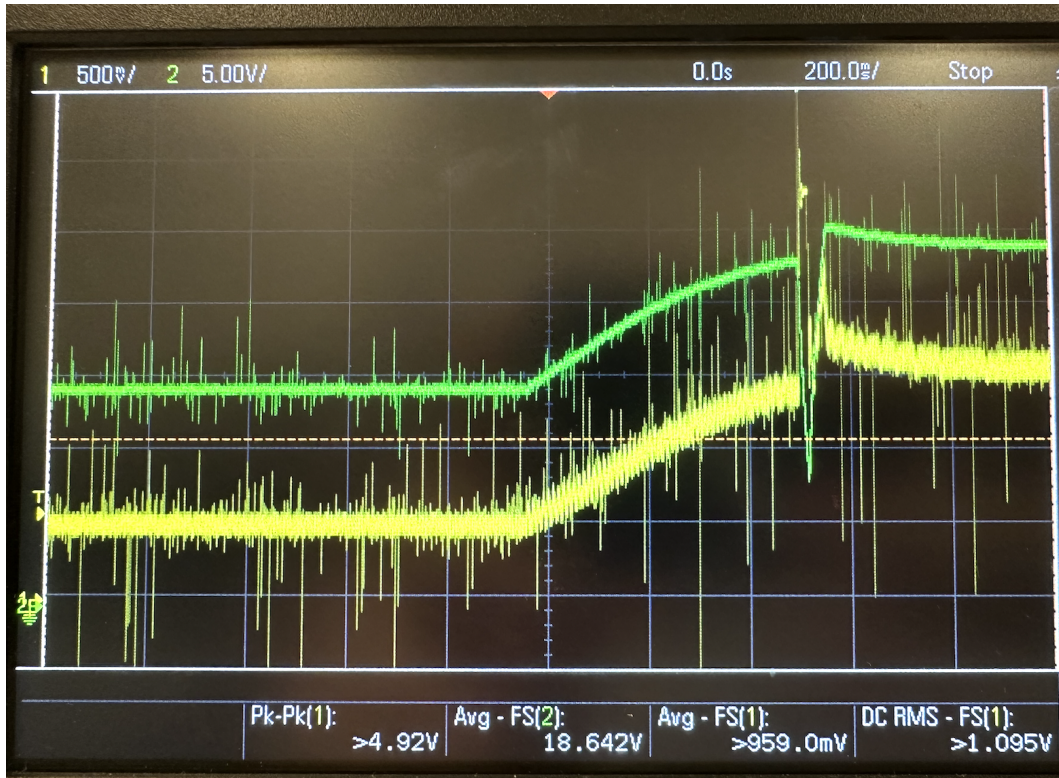


Figure 7: Transient captured of output voltage (green) and duty cycle (yellow) as pin 8 was switched from ground to 3.3 V

From Figure 7, when pin 8 is switched from ground to 3.3 V, the duty cycle waveform rises to increase the output voltage from 15 V to 25 V. This is the expected behavior of the feedback circuit. Since the integral gain is low, there is a smooth transition between the two voltage levels and duty cycle levels. The large spike at the end of the transition can be attributed to unattenuated noise in the circuit or unfiltered high frequency transients. Ignoring that spike, the circuit and feedback behave as expected.

Next, the transient for switching the 50Ω load on is observed. When the 50Ω load is added in parallel, the load current increases causing more stress on the circuit. The result of this is observed in Figure 8.

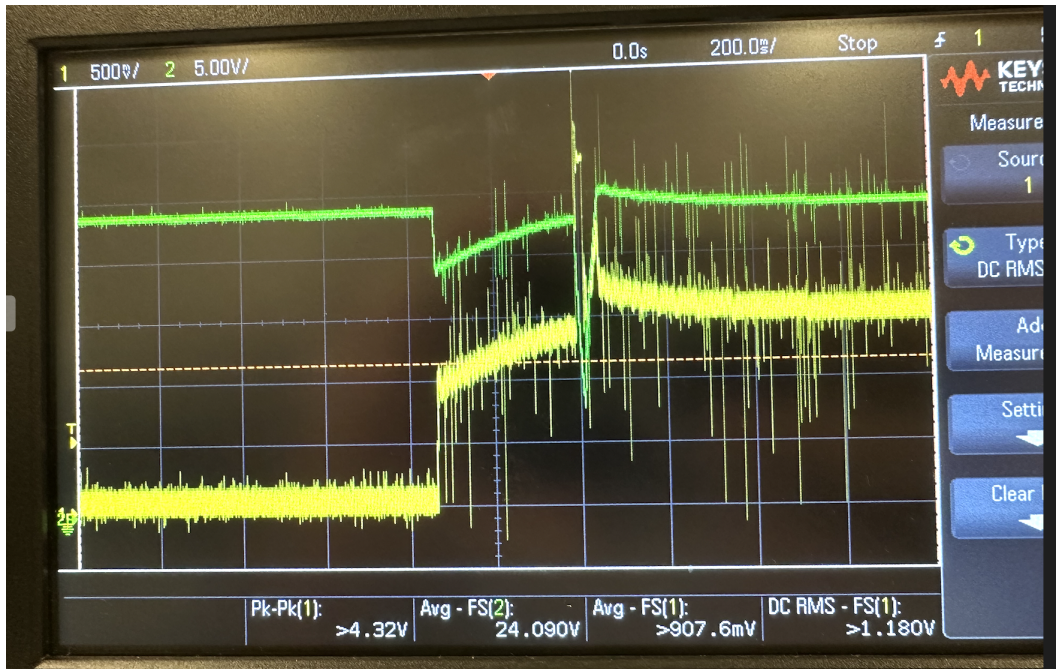


Figure 8: Transient captured of output voltage (green) and duty cycle (yellow) as 50Ω load is added in parallel

From Figure 8, when the 50Ω load is added in parallel, the circuit is stressed and the output voltage drops. Through the feedback, the PID control raises the duty cycle to compensate and the output voltage returns to the original

level of 25 V. Once again, the large spike at the end of the transition can be attributed to unattenuated noise in the circuit or unfiltered high frequency transients. Ignoring that spike, the circuit and feedback behave as expected.

Lastly, the controller was reprogrammed with a high integral gain of $K_i = 200$ and command voltage set to 25 V. This result is shown in Figure 9.



Figure 9: Output voltage waveform (green) vs duty cycle (yellow) for $K_i = 200$

From Figure 9, the output voltage waveform exhibits instability as a result of the high integral gain. The controller initially drives the duty cycle to its maximum in an effort to reach the 25 V target. Once the output reaches the setpoint, the controller sharply reduces the duty cycle to its minimum in an attempt to prevent overshoot. This aggressive back-and-forth response leads to a sustained oscillation in the output voltage. While an ideal system might experience diverging oscillations, the real system is limited by hardware constraints, causing the output to swing between upper and lower bounds

rather than increasing indefinitely.

9 Conclusion

Simulations showed strong agreement with calculated values, particularly for inductor current and efficiency. Voltage error became more significant when inductor resistance was neglected, especially in DCM and at higher load resistances. When inductor resistance increased to 1.5Ω , voltage drop and efficiency decreases were observed in both simulations and measurements.

Experimental results validated the simulation and theoretical models, with measured current and efficiency aligning closely across all cases. The effect of core saturation was also captured at high load current conditions.

Transient analysis of the microprocessor-controlled feedback system confirmed expected behavior. The feedback controller responded correctly to voltage setpoint changes and load variations. With a high integral gain ($K_i = 200$), the output became unstable, oscillating between duty cycle extremes.